Improving Satellite-Derived Sea Surface Temperature Accuracies Using Water Vapor Profile Data

IAN J. BARTON

CSIRO Marine and Atmospheric Research, Hobart, Tasmania, Australia

(Manuscript received 31 May 2010, in final form 30 August 2010)

ABSTRACT

Analyses based on atmospheric infrared radiative transfer simulations and collocated ship and satellite data are used to investigate whether knowledge of vertical atmospheric water vapor distributions can improve the accuracy of sea surface temperature (SST) estimates from satellite data. Initially, a simulated set of satellite brightness temperatures generated by a radiative transfer model with a large maritime radiosonde database was obtained. Simple linear SST algorithms are derived from this dataset, and these are then reapplied to the data to give simulated SST estimates and errors. The concept of water vapor weights is introduced in which a weight is a measure of the layer contribution to the difference between the surface temperature and that measured by the satellite. The weight of each atmospheric layer is defined as the layer water vapor amount multiplied by the difference between the SST and the midlayer temperature. Satellite-derived SST errors are then plotted against the difference in the sum of weights above an altitude of 2.5 km and that below. For the simple two-channel (with typical wavelengths of 11 and 12 μm) analysis, a clear correlation between the weights differences and the SST errors is found.

A second group of analyses using ship-released radiosondes and satellite data also show a correlation between the SST errors and the weights differences. The analyses suggest that, for an SST derived using a simple two-channel algorithm, the accuracy may be improved if account is taken of the vertical distribution of water vapor above the ocean surface. For SST estimates derived using algorithms that include data from a 3.7-μm channel, there is no such correlation found.

1. Introduction

Sea surface temperature (SST) is one of the basic parameters in the research and prediction of climate variability and change. Recent global measurements have been supplied by both in situ and satellite-borne instruments, and these continue today. Space-based estimates of SST have been supplied by a continuous constellation of meteorological satellites launched initially by the United States, and more recently by other national and international space agencies. The first of these satellites was Television and Infrared Observation Satellite (TIROS)-N, launched in 1979, which included the Advanced Very High Resolution Radiometer (AVHRR) with two infrared channels used to give surface and cloud-top temperatures. Later versions of the AVHRR included three infrared channels for improved surface temperature measurement. The basic three channels for SST derivation have central wavelengths close to 3.7, 10.8, and 12.0 μm, and differential absorption techniques are used to provide a correction for atmospheric water vapor absorption. One of the first theoretical analyses of satellite-derived SST was presented in the classical paper of McMillin (1975).

The derivation of SST from infrared satellite data first requires ''cloud detection'' to ensure that there is a clear view of the surface. Cloud detection is more reliable during the daytime when the shortwave visible and near-infrared channels of the AVHRR can be used to detect reflected sunlight. Use of the 3.7-μm data is limited to the night because there is a significant reflected solar contribution that is added to the surface-emitted infrared component during the day. Thus, the standard SST retrieval from AVHRR is provided by using the two thermal infrared channels at 11 and 12 μm. Following the theoretical analysis of McMillin (1975), a simple linear multichannel SST (MCSST), based on empirical regression with satellite and in situ data, was developed by McClain et al. (1985)

Corresponding author address: Ian J. Barton, P.O. Box 1538, Hobart, Tasmania 7001, Australia.
E-mail: ian.barton@csiro.au

DOI: 10.1175/2010JTECHA1502.1

and used operationally with data from the AVHRR. A review of current satellite-derived SST was presented by Barton (1995), which listed typical accuracies close to 0.6 K for using AVHRR data. Further improvements in SST accuracy were obtained using nonlinear SST (NLSST) algorithms as developed by Walton et al. (1998). They used a radiative transfer model to show that if a term based on an independent measurement or estimation of SST was included in an MCSST algorithm, then the SST accuracy was improved to 0.5 K. More recent work reported by Merchant et al. (2008) using optimal estimation (OE) techniques has further improved the SST accuracy to less than 0.5 K.

As well as atmospheric absorption, there are two ocean surface phenomena that must be considered when comparing SST estimates. Evaporative and radiative cooling of the ocean surface give a thin (tens of micrometers) cool skin surface layer under almost all conditions. Donlon et al. (2002) suggest that a typical value of the bulk–skin temperature difference is 0.17 K, but variability resulting from many physical factors is likely. The second phenomenon is linked to solar heating of the near-surface layers (tens of centimeters) under light wind conditions (<6 m s^{-1}). Much research work is now addressing these issues in an attempt to either measure or predict the temperature structure of the upper meter of the ocean. Finally, Minnett and Barton (2010) give an up-to-date summary of the current status of retrieving SST from satellite measurements.

The National Oceanic and Atmospheric Administration (NOAA) orbiting meteorological satellites also include the High Resolution Infrared Radiation Sounder (HIRS) instrument, which is designed to give vertical profiles of temperature and water vapor beneath the satellite. These measurements complement those from the AVHRR and allow the general use of several data products in meteorological forecasting. Several papers have suggested the use of water vapor estimates in the derivation of SST to improve the retrieval accuracy (Emery et al. 1994; Sobrino et al. 1994), but these have all been restricted to the use of total column water vapor (TWV) and not the use of any profile (vertical) information. Nalli and Smith (1998) and others have used water vapor profiles in the physical retrieval of SST, but these techniques require a full radiative transfer calculation for each retrieval. In this paper a means of including water vapor *profile* data in simple empirical SST retrievals is developed. The new technique is shown to improve the two-channel SST accuracy for AVHRR and other infrared radiometers. Given that the majority of SST estimates in the historical archive are from the 11- and 12-μm channels of the AVHRR and other instruments, this will give a significant improvement to the accuracy of the SST archive. Details of all the satellite instruments used in this study are easily available on the Internet.

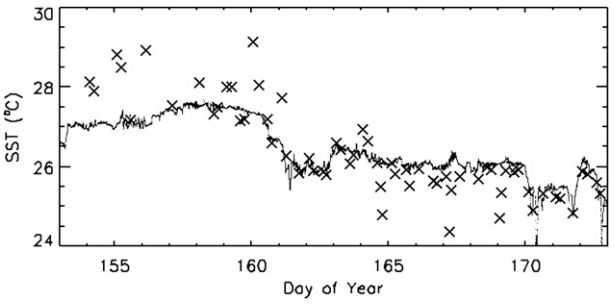

FIG. 1. Results of the SST comparisons from the ship and satellite data collected off the northwest coast of Australia during June 2006. The SST from the ship thermosalinograph (solid lines) and the SST derived from AVHRR data (crosses) are shown.

2. Previous work

Early papers by Barton (1995, 1998) have discussed the use of some vertical water vapor estimates to improve the SST retrieval from satellite radiometers. A theoretical analysis in the second paper demonstrated an improved accuracy if the water vapor content above 3 km was known. The application of this technique has not been implemented because of the past difficulty of obtaining water vapor profile estimates coincident with the infrared satellite data, and the need for the increased accuracy.

A renewed interest in this topic has come from the analysis of a dataset collected on the Research Vessel (R/V) *Southern Surveyor* operating on the North West shelf off the northwest coast of Australia (16°–20°S, 118°–122°E). During June 2006 ship measurements of SST were made with a thermosalinograph and an infrared radiometer as part of the geophysical validation campaign for the Advanced Along-Track Scanning Radiometer (AATSR) on the *Environmental Satellite* (*Envisat*). These ship-borne measurements were compared with SST derivations from several satellite-borne radiometers, including the AVHRR instruments on the *NOAA-17* and *-18* meteorological satellites. The results were reported by Barton (2007) to the *Envisat* Symposium held at Montreux, Switzerland. A graph showing a comparison between the SSTs measured by the ship's thermosalinograph and those derived from the AVHRR is included as Fig. 1. The figure shows that, prior to day 162, many of the AVHRR SST estimates were significantly higher than the ship measurements, while after day 162 the satellite estimates were less than those from the ship.

The data plots in Barton (2007) show that between days 153 and 162 the daytime surface wind speed exceeded 10 m s^{-1}, except on day 155 when it was around 5 m s^{-1}. Following day 164 the wind speed exceeded 6 m s^{-1} except for days 166–168. The data plots also include SST measurements from the thermosalinograph and ship-borne infrared radiometer, and these show no diurnal warming during the first period, but some minor warming during days 166–168. On these latter days Fig. 1 shows no evidence of increased AVHRR SSTs, which would be expected with diurnal warming. These data thus suggest that the differences between the AVHRR and the ship measurements of SST are not due to diurnal warming effects.

A further analysis of the surface relative humidity (SRH) measured on the ship and the TWV measured by the Advanced Microwave Scanning Radiometer for Earth Observing System (EOS; AMSR-E) on the *Aqua* satellite suggested that, prior to day 162, there was considerable water vapor in the upper atmosphere (TWV = 30–36 mm, SRH = 45%–60%), but a lack of upper-level water vapor in the period following this day (TWV < 20 mm, SRH = 40%–65%). It will be shown in this work that these observations agree with an analysis using simulated satellite data as well as an analysis of *NOAA-18* HIRS data obtained for this period and location during June 2006.

3. Development of the method—Simulated data analysis

The thesis explored in this paper is that atmospheres with abnormal vertical structures of water vapor can give erroneous estimates of SST when a first-guess water vapor profile is usually assumed. This assumption is implicit with the development of all currently used algorithms, whether they are derived using matching buoy and satellite brightness temperatures, or a multiple regression analysis with transmission model-derived brightness temperatures.

The derivation of SST from infrared observations relies on the differential absorption of the atmosphere at different wavelengths. Those wavelengths used for SST derivation are in the thermal infrared between 3 and 13 μm. In this spectral region, in tropical and midlatitude climates, the main absorbing atmospheric constituent is water vapor. Infrared radiation emitted from the surface is absorbed and scattered by the atmosphere, and some radiation is reemitted at the (cooler than the surface) temperature of the atmosphere. The net result is that the radiance reaching a satellite radiometer is less than that emitted by the surface. The apparent brightness temperature (BT) measured by the satellite is less than the surface temperature and the difference is usually called the temperature deficit (ΔT),

$$\Delta T = \mathrm{SST} - \mathrm{BT}. \tag{1}$$

The deficit ΔT, at each wavelength, is determined by the amount of water vapor (WV) in the atmosphere and the difference between the surface and WV temperatures. WV that has the same temperature as the SST makes no contribution to ΔT because the absorbed and reemitted radiances are equal, while WV that is much colder than the SST makes a significant contribution to the ΔTs, which are thus determined by the WV concentration in the atmosphere and its temperature relative to the SST. At 11 μm (say), where the WV absorption is less than at 12 μm, the contribution of the upper-level WV is considerable because the lower-level WV does not significantly reduce the upwelling radiance. In contrast, at 12 μm, the lower-level WV absorption is considerable and there is less radiance available for absorption by the upper-level WV. The thesis of this work is that the difference in the relative amounts of absorption at the lower and upper atmospheric levels will introduce errors in SST analyses based on empirical algorithms that do not take account of any vertical water vapor structure. Now, by dividing the atmosphere (surface to a height of 10 km) into 20 equal height layers it is possible to determine the contribution of each layer to ΔT. WV amounts above 10 km are extremely small and make little contribution to ΔT. To quantify this process the concept of WV weights (WW) is introduced, where

$$\mathrm{WW}_n = \mathrm{WV}_n(\mathrm{SST} - T_n). \tag{2}$$

Here n is the layer number, WV_n is the precipitable WV amount in layer n, SST is the near-surface temperature in the radiosonde data, and T_n is the temperature at the middle of the layer.

This concept is investigated further by using the *Diamantina* and *Gascoyne* (DIGA) vessels maritime radiosonde dataset of 885 profiles (Baker and Dowd 1978). These data were collected by two Royal Australian Navy vessels using Philips RS4 radiosondes and cover the area bounded by 10°N–50°S latitude and 90°E–180° longitude. The water vapor amounts WV_n in each 500-m layer from the surface to 10 km and the midlayer temperatures T_n are extracted using linear interpolation. Weights for each layer are then calculated as above and are then summed to give total weights for 0–2.5 and 2.5–10 km. The height of 2.5 km is selected because this gives approximately average equal sums of weights above and below this level. Other heights were examined, but none produced any improvement in the results. However, it is expected that in the future more detailed analyses with selected datasets may give different optimum heights depending on climate, location, and the local weather situation. The two sums are given by

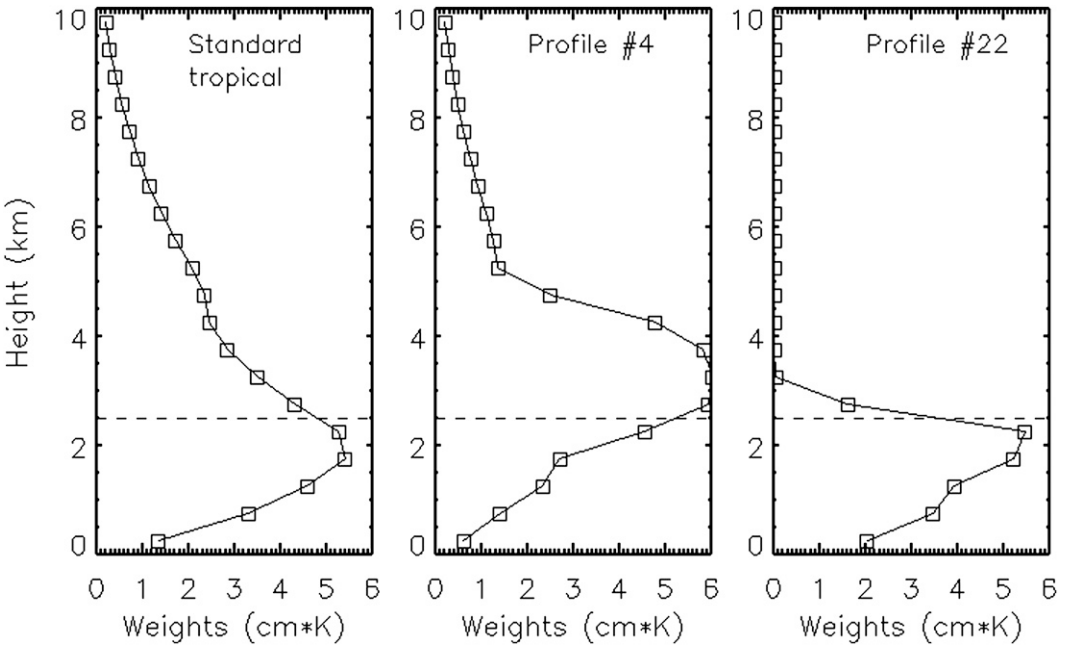

FIG. 2. WV weights for three different atmospheres. Weights sums and sum differences ($\Sigma\{WW\}_{6-20}$, $\Sigma\{WW\}_{1-5}$ and $\Sigma\{WW\}_{6-20} - \Sigma\{WW\}_{1-5}$) for each profile are (left) (24, 20, 4), (middle) (35, 12, 23), and (right) (1, 20, −19).

$$WW(0 - 2.5\,km) = \Sigma\{WW\}_{1-5} \quad \text{and} \tag{3}$$

$$WW(2.5 - 10\,km) = \Sigma\{WW\}_{6-20}. \tag{4}$$

Weights are shown for three different atmospheres in Fig. 2: a standard tropical atmosphere, one with a significant amount of WV above 2.5 km, and one with no WV above 3 km. The figure caption gives the two WW sums and the sum differences (WWdiff) for each profile.

The following linear, ATSR-like, SST algorithms [$SST = C_0 + \Sigma C_n(BT_n)$] are developed from the set of simulated brightness temperatures derived for the DIGA radiosonde dataset by Owen Embury and Chris Merchant at The University of Edinburgh (2007, personal communication) using the latest version of their atmospheric transmission model (Merchant et al. 1999):

(i) SST(2 channels) 11- and 12-μm nadir view;
(ii) SST(3 channels) 3.7-, 11-, and 12-μm nadir view;
(iii) SST(2 channels, dual view) 11- and 12-μm nadir and forward views;
(iv) SST(3 channels, dual view) 3.7-, 11-, and 12-μm nadir and forward views.

These linear algorithms are reapplied to the brightness temperature dataset to give estimates of the SST, and these are compared with the original SST value in the radiosonde dataset. Finally, the SST errors are plotted against the following parameters for each of the four algorithms above:

(i) $WWdiff = \Sigma\{WW\}_{6-20} - \Sigma\{WW\}_{1-5}$ Difference,
(ii) $WWratio = \Sigma\{WW\}_{6-20}/\Sigma\{WW\}_{1-5}$ Ratio,
(iii) $WWdiff n = [\Sigma\{WW\}_{6-20} - \Sigma\{WW\}_{1-5}]^n$ $n = 0.5$ to 2.0,
(iv) median height of WV.

The plots demonstrate that the best correlation between SST errors (two channels) and water vapor distribution is for the simple weights difference (WWdiff) shown in Fig. 3a. The procedure is repeated for 200-m layers, but no improvement is noticed. The plots also show no obvious correlation for three-, four-, and six-channel algorithms with Fig. 3b showing the plot for the four-channel algorithm.

Simple linear statistics are derived for the data shown in Fig. 3a and are included in Table 1. A good correlation is found when the TWV content is less than 4.5 cm. For moist tropical atmospheres when the TWV is greater than 4.5 cm, the correlation, for this dataset, is poor. Note, however, that some later analyses with nonsimulated data do give some correlation for those coincidences with TWV > 4.5 cm. For TWV amounts less than 4.5 cm, the correlation between SST error and WWdiff is given by

$$SST\ error = -0.027(WWdiff) - 0.10. \tag{5}$$

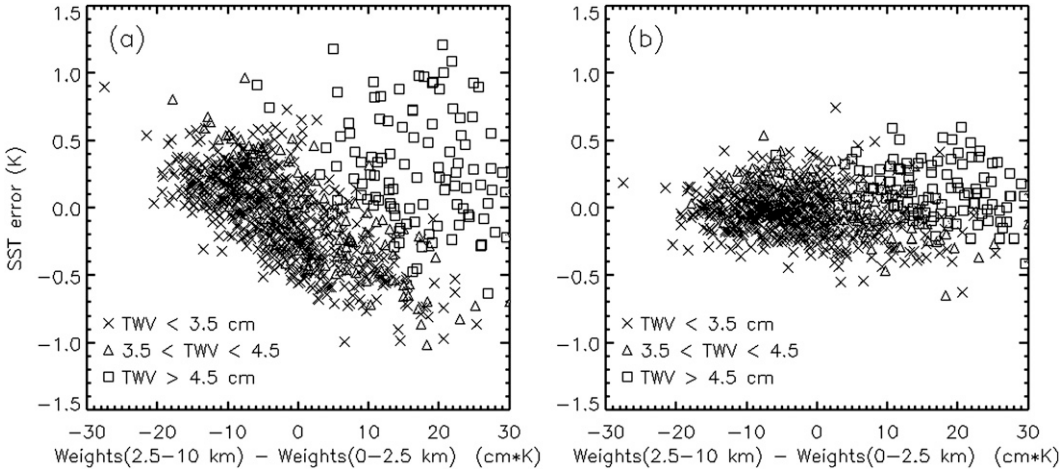

FIG. 3. SST error plotted against WWdiff for a derivation of SST with the simulated BT dataset from the DIGA radiosonde data: (a) two-channel and (b) four-channel algorithms are shown.

This implies that the two-channel algorithm gives an SST error of close to 0.5 K when the magnitude of WWdiff is 20 cm K^{-1}.

4. Satellite data analyses

a. North West shelf analysis

Comparisons between the R/V *Southern Surveyor* and satellite measurements for June 2006 are shown in Fig. 1. These results have been presented by Barton (2007) and include some approximate estimates of vertical water vapor distribution derived from surface humidity measurements on the research vessel and TWV estimates from the AMSR-E, which is part of the payload of the *Aqua* satellite. Since this early analysis further data from the HIRS instrument on the *NOAA-18* satellite have been provided by NOAA. Analysis of these data, to provide WV and temperature distributions with height, confirms the different atmospheric conditions before and after day 164 of 2006 (see Fig. 4). It is interesting to note that the absolute magnitudes of WWdiff from the HIRS analysis are somewhat less that those obtained from the simulated data analysis, perhaps suggesting that the HIRS sounding analysis may be biased toward ''average'' atmospheric structure when applied to anomalous vertical profiles.

b. M-AERI–AATSR analysis

Between 2001 and 2006 the University of Miami deployed a Marine-Atmospheric Emitted Radiance Interferometer (M-AERI; see Minnett et al. 2001 for details) on the cruise ship *Explorer of the Seas* (Williams et al. 2002). This ship made weekly cruises from Miami, Florida, to the Caribbean Sea, and the main aim of the interferometer deployment was to validate the SST estimates derived from the Moderate Resolution Imaging Spectroradiometer (MODIS) instruments on the *Terra* and *Aqua* satellites. As part of the data collection system radiosondes were regularly launched from the ship at times of satellite overpasses. This large unique dataset has been made available to assist with this study. The data have also been made available to The University of Leicester to assist in the validation of the SST estimates from the AATSR instrument. Again, the AATSR data that match the *Explorer of the Seas* radiosonde dataset have been made available by the University of Leicester and are also used in the following analysis (see Noyes et al. 2006 for details).

All of the radiosonde data are processed to supply WWdiff values for comparison with the SST validation results. Radiosonde data were usually collected at MODIS overpass times and, for the *Aqua* instrument, these could be different to AATSR times by up to 4 h. The surface SST measurements by the M-AERI were restricted to be within 2 h of the AATSR overpass times giving 96 sets of data. For the 4-h window each of these datasets could contain up to 16 M-AERI SST measurements at different locations along the ship's track. From the University of Leicester dataset the AATSR data for each

TABLE 1. Correlation statistics for the two-channel algorithm results in Fig. 3a.

TWV range (cm)	*N*	Intercept	Slope	RMS (K)
0.0–7.0	885	0.00	−0.010	0.35
0.0–4.5	770	−0.10	−0.027	0.24
0.0–3.5	659	−0.13	−0.028	0.23

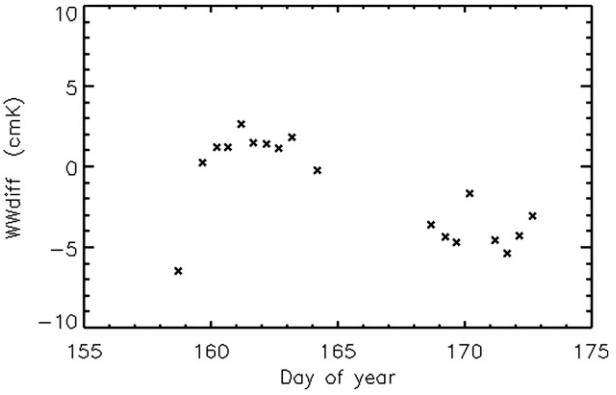

FIG. 4. Water vapor weights differences derived from the HIRS instrument on the *NOAA-18* satellite for the North West shelf during June 2006 (cf. Fig. 1).

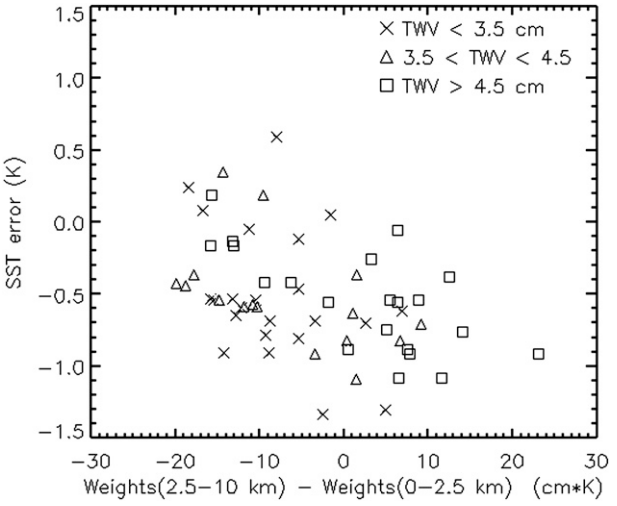

FIG. 5. SST error for a two-channel AATSR SST derivation plotted against WWdiff derived from the *Explorer of the Seas* radiosonde data. Number of data points N is 64.

location in each dataset are extracted for a single pixel and 3×3 and 5×5 pixel arrays. Finally, for each radiosonde the coincident AATSR data with the minimum range of nadir 3×3 pixel 11-μm BT is selected for comparison with the coincident M-AERI SST. To eliminate possible cloud-contaminated data, those coincidences with 11-μm BT ranges greater than 0.5 K are rejected (64 remained). The results of comparing the SST error (difference between M-AERI and AATSR) and WWdiff are shown in Fig. 5.

In this AATSR–radiosonde analysis the results show a linear correlation for all values of TWV, in contrast to the simulated results in which no correlation is found for TWV $>$ 4.5 cm. The results give the following dependence:

$$\text{SST error} = -0.025(\text{WWdiff}) - 0.58 \quad (\text{RMS } 0.53), \tag{6}$$

which is in close agreement with the simulated expression given above [Eq. (5)]. This limited dataset also suggests that, in the Caribbean Sea, the AATSR SSTs are on average 0.5 K colder than those measured by the M-AERI.

c. M-AERI–MODIS analysis (Explorer of the Seas)

The *Explorer of the Seas* dataset supplied by the University of Miami includes SST estimates from the MODIS instruments on *Aqua* and *Terra*. The dataset contains 705 radiosonde flights and 15 905 comparisons between the M-AERI and MODIS estimates of SST. To ensure a good matchup dataset between the radiosonde and interferometer measurements, the databases are filtered to restrict the time difference to be less than 1 h, and both the latitude and longitude differences to be less than 0.5°. The standard deviation of the MODIS SSTs in a 3×3 pixel area around the central pixel is also restricted to be less than 0.5 K to ensure that only the highest quality, cloud-free data are used in the analysis. After these restrictions are applied there are 457 coincidences remaining. The results are shown in Fig. 6 and the linear statistical parameters are included later in Table 2.

d. M-AERI–MODIS analysis (non–Explorer of the Seas data)

The M-AERI and radiosonde data were also collected from several other vessels to provide a wider geographic coverage for the validation of SST estimates from the two MODIS instruments. These include 709 radiosonde ascents and 3794 comparisons between ship and MODIS measurements of SST. The same restrictions are applied to the data as with those from *Explorer of the Seas*, leaving a total of 75 coincidences. This total is reduced to 68 when those with TWV $>$ 4.5 cm are removed. Again, the SST errors derived from MODIS data are plotted against the WWdiff values from the radiosonde data. The results are shown in Fig. 7 with correlation statistics (in Table 2), similar to the *Explorer of the Seas* data for both all TWV values and those with TWV $<$ 4.5 cm.

e. Skin–bulk differences and diurnal warming issues

The analyses undertaken above are all independent of skin–bulk temperature differences and diurnal warming effects. For the simulated data analysis, neither of these phenomena is an issue. For the AATSR–M-AERI analysis, both the AATSR SST algorithm and the M-AERI give a measurement of skin SST. With the remaining analyses the MODIS SST algorithm gives a bulk SST that is close to 0.2 K warmer than the skin SST measured by

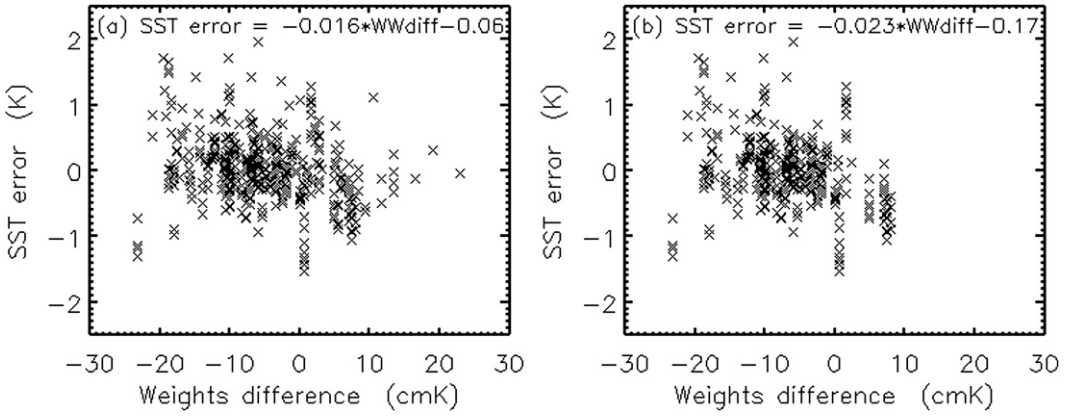

FIG. 6. SST errors from the MODIS validation database plotted against WWdiff for *Explorer of the Seas* radiosonde data: (a) for all data ($N = 457$) and (b) for data with TWV ≤ 4.5 cm ($N = 363$).

the M-AERI (Donlon et al. 2002). This will introduce a small offset in the intercept of the linear relation between the SST error and WWdiff but will not affect the slope.

With diurnal warming present, both the M-AERI and the satellite radiometers will provide an elevated surface temperature, but the relation between SST error and WWdiff will not be affected.

f. Summary of the results

The results found for both the simulated and empirical data analyses are listed in Table 2. Important parameters to observe in the table are the ''Slope,'' which relates the SST error to the WWdiff, and the difference between the two RMS values, which shows the advantage of applying the weights analysis. In each of the analyses given the intercept shows variation resulting from several factors: whether the skin or bulk SST as measured by the ship instruments is used, the magnitude of the coefficients of the SST algorithm, and whether the average state of the atmosphere gives equal WW sums above and below an altitude of 2.5 km. Studies with long-term datasets will ultimately provide optimum slope and offset parameters for each region and algorithm.

The analyses suggest that, for atmospheres with TWV < 4.5 cm, a slope (SST error/WWdiff) close to −0.025 should be adopted. For anomalous atmospheres with a WWdiff magnitude of 20 cm K^{-1}, as shown in Fig. 3a, this implies an SST error (true SST minus satellite-derived SST) of −0.5 K. In this case a simple adjustment of reducing the satellite-derived SST by 0.5 K would provide a more accurate value.

Current analyses of AVHRR 11- and 12-μm data are undertaken using an NLSST algorithm that includes a term equal to a constant multiplied by an external estimate of the SST (Walton et al. 1998). In some ways this term can also be seen as a proxy for latitude or TWV. Given that the NLSST is still based on the difference between the two brightness temperatures, and that no account is taken of the vertical WV profile, the application of WWdiff would appear to produce similar results as presented above.

The simulated data analyses show a definite improvement in the SST estimates of close to 0.1 K when the weights analysis is applied. For the empirical studies the improvement is not as great, being between 0.00 and 0.05 K. These empirical analyses have been undertaken

TABLE 2. Correlation statistics for the various analyses. The original RMS and the RMS are the standard errors before and after the weights analysis was applied to the data. It is important to note that the RMS values given here only apply to simple two-channel SST algorithms.

Data source	TWV range	*N*	Intercept	Slope	RMS (K)	Original RMS (K)
Theoretical	All	885	0.00	−0.010	0.35	0.36
	≤4.5 cm	770	−0.10	−0.027	0.24	0.33
AATSR and *Explorer of the Seas* radiosondes	All	64	−0.58	−0.025	0.53	0.58
	≤4.5 cm	43	−0.68	−0.033	0.62	0.67
MODIS and *Explorer of the Seas* radiosondes	All	457	−0.06	−0.016	0.50	0.52
	≤4.5 cm	363	−0.17	−0.023	0.51	0.53
MODIS and non–*Explorer of Seas* radiosondes	All	75	0.33	−0.011	0.49	0.49
	≤4.5 cm	68	0.28	−0.021	−0.021	0.44

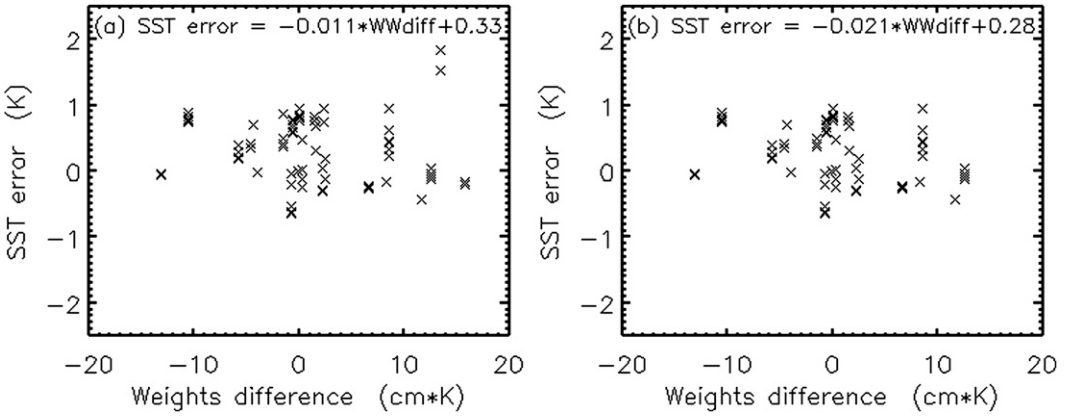

FIG. 7. SST errors from the MODIS validation database plotted against WWdiff for the radiosondes launched from vessels other than *Explorer of the Seas*: (a) for all data ($N = 75$) and (b) for data with TWV $\leq$ 4.5 cm ($N = 68$).

on small datasets with limited data quality assessment. Further studies will be required to determine whether the advantages suggested in the simulated data analyses can be translated to future operational data analyses and the reprocessing of existing datasets.

5. Conclusions

Numerically simulated and empirical data analyses have demonstrated a relation between errors in satellite-derived SST estimates and the vertical water vapor structure of the overlying atmosphere. A new parameter has been developed that gives an estimate of the effect of the water vapor structure on the SST derivation. The atmosphere has been divided into layers, with each layer WV amount being multiplied by the difference between the surface and midlayer temperatures to give a WV weight. This parameter is basically the contribution of the infrared absorption of the layer to the difference between the SST and the brightness temperature measured at the satellite. Summing the weights above and below a nominated height (here 2.5 km is used) gave a difference parameter that was directly related to the error in the determination of SST using a simple two-channel (wavelengths of 11 and 12 μm) SST algorithm. The arbitrarily selected height of 2.5 km may not be the optimum height for future analyses, and this height may vary with climate and location. Only a more rigorous data analysis on larger datasets than those made available for this study will determine the optimum height for determining WWdiff.

The relation between WWdiff and SST error was only found for the simple two-channel 11- and 12-μm derivation as used by AVHRR, MODIS, and AATSR during both the daytime and at night. No significant effect was noticed when the 3.7-μm or dual-view data were used in algorithms to derive the SST. With the simulated data analysis the method failed for very moist atmospheres with TWV $>$ 4.5 cm, but appeared to work for moist atmospheres when applied to the *Explorer of the Seas* radiosondes and collocated AATSR data.

The analysis has also been applied to datasets provided by the Universities of Miami and Leicester. These included radiosondes and M-AERI data from the *Explorer of the Seas*, along with coincident AATSR data, generally within a time window of less than 4 h. For AATSR two-channel SSTs there was no high TWV limit, as stated above, for the simulated data analysis.

Both the simulated and empirical data analyses confirmed that SST estimates using a simple two-channel algorithm could be improved by taking account of the vertical structure of water vapor, although the improvement was greater in the simulated data analysis. To enable this enhancement in SST derivation, a means for determining WV weights using both satellite measurements and weather forecast analyses on a global scale should be implemented. Corrections to most two-channel SST estimates could then be made globally. The long-term SST dataset, provided by infrared radiometers on satellites, contains many early measurements based on simple 11- and 12-m data. A reanalysis taking account of vertical WV distributions will thus enhance the accuracy of this dataset and its use in climate change studies.

Acknowledgments. Stephen Thomas and the captain and crew of the R/V *Southern Surveyor* provided the in situ data in the Bonaparte Gulf. Owen Embury and Chris Merchant, at the University of Edinburgh, have supplied the simulated BT data from the DIGA radiosonde dataset. Gary Corlett, at the University of Leicester, has provided the AATSR dataset to match the M-AERI and radiosonde data from the *Explorer of the Seas*. Peter Minnett and others at the University of Miami kindly

supplied all of the ship and radiosonde data for the MODIS validation campaign both from the *Explorer of the Seas* and many other vessels. The collection of these latter datasets has been funded by NASA and NOAA.

REFERENCES

Baker, P. W., and A. M. Dowd, 1978: The occurrence of radio ducting, superrefractive and subrefractive conditions in Australian maritime regions. Electronics Research Laboratory, Defence Science and Technology Organisation, Department of Defence, Tech. Rep. ERL-0048-TR, 26 pp and 9 figs.

Barton, I. J., 1995: Satellite-derived sea surface temperatures: Current status. *J. Geophys. Res.,* **100,** 8777–8790.

——, 1998: Improved techniques for derivation of sea surface temperatures from ATSR data. *J. Geophys. Res.,* **103,** 8139–8152.

——, 2007: Satellite-derived sea surface temperatures—A case study of error variability. *Proc. ENVISAT Symp. 2007,* ESA SP-636, Montreux, Switzerland, ENVISAT. [Available online at http://envisat.esa.int/envisatsymposium/proceedings/sessions/5C1/507309ba.pdf.]

Donlon, C. J., P. J. Minnett, C. Gentemann, T. J. Nightingale, I. J. Barton, B. Ward, and M. J. Murray, 2002: Toward improved validation of satellite sea surface skin temperature measurements for climate research. *J. Climate,* **15,** 353–369.

Emery, W. J., Y. Yu, G. A. Wick, P. Schluessel, and R. W. Reynolds, 1994: Correcting infrared satellite estimates of sea surface temperature for atmospheric water vapor attenuation. *J. Geophys. Res.,* **99,** 5219–5236.

McClain, E. P., W. G. Pichel, and C. C. Walton, 1985: Comparative performance of AVHRR-based multichannel sea surface temperatures. *J. Geophys. Res.,* **90,** 11 587–11 601.

McMillin, L. M., 1975: Estimation of sea surface temperatures from two infrared window measurements with different absorption. *J. Geophys. Res.,* **80,** 5113–5117.

Merchant, C. J., A. R. Harris, M. J. Murray, and A. M. Zavody, 1999: Toward the elimination of bias in satellite retrievals of sea surface temperature 1. Theory, modeling and interalgorithm comparison. *J. Geophys. Res.,* **104,** 23 565–23 578.

——, P. LeBorgne, A. Marsouin, and H. Roquet, 2008: Optimal estimation of sea surface temperature from split-window observations. *Remote Sens. Environ.,* **112,** 2469–2484.

Minnett, P. J., and I. J. Barton, 2010: Remote sensing of the earth's surface temperature. *Radiometric Temperature Measurements and Applications,* Z. M. Zhang, B. K. Tsai, and G. Machin, Eds, Academic Press/Elsevier, 333–391.

——, R. O. Knuteson, F. A. Best, B. J. Osborne, J. A. Hanafin, and O. B. Brown, 2001: The Marine-Atmospheric Emitted Radiance Interferometer (M-AERI), a high-accuracy, sea-going infrared spectroradiometer. *J. Atmos. Oceanic Technol.,* **18,** 994–1013.

Nalli, N. R., and W. L. Smith, 1998: Improved remote sensing of sea surface skin temperature using a physical retrieval method. *J. Geophys. Res.,* **103,** 10 527–10 542.

Noyes, E. J., P. J. Minnett, J. J. Remedios, G. K. Corlett, S. A. Good, and D. T. Llewellyn-Jones, 2006: The accuracy of the AATSR sea surface temperatures in the Caribbean. *Remote Sens. Environ.,* **101,** 38–51.

Sobrino, J. A., Z.-L. Li, and M. P. Stoll, 1994: Impact of the atmospheric transmittance and total water vapor content in the algorithms for estimating satellite sea surface temperatures. *IEEE Trans. Geosci. Remote Sens.,* **31,** 946–952.

Walton, C. C., W. G. Pichel, J. F. Sapper, and D. A. May, 1998: The development and operational application of nonlinear algorithms for the measurement of sea surface temperatures with the NOAA polar-orbiting environmental satellites. *J. Geophys. Res.,* **103,** 27 999–28 012.

Williams, E., E. Prager, and D. Wilson, 2002: Research combines with public outreach on a cruise ship. *Eos, Trans. Amer. Geophys. Union,* **83,** 590–596.